eNeuro

Research Article: Negative Results | *Disorders of the Nervous System*

No detectable effect on visual responses using functional MRI in a rodent model of α-synuclein expression

https://doi.org/10.1523/ENEURO.0516-20.2021

Cite as: eNeuro 2021; 10.1523/ENEURO.0516-20.2021

Received: 30 November 2020
Revised: 23 April 2021
Accepted: 30 April 2021

Title: No detectable effect on visual responses using functional MRI in a rodent model of α-synuclein expression

Abbreviated title: fMRI of α-synuclein model of Parkinson's Disease

Freja Gam Østergaard[1], Christian Stald Skoven[3], Alex R. Wade[2], Hartwig R. Siebner[3], Bettina Laursen[1], Kenneth Vielsted Christensen[1], Tim B. Dyrby[3,4]

[1] Circuit Biology, H. Lundbeck A/S, Ottiliavej 9. DK-2500 Valby, Denmark.
[2] Department of Psychology, The University of York, Heslington, York, YO10 5DD, United Kingdom.
[3] Danish Research Centre for Magnetic Resonance, Centre for Functional and Diagnostic Imaging and Research, Copenhagen University Hospital - Amager and Hvidovre, Copenhagen, Denmark
[4] Department of Applied Mathematics and Computer Science, Technical University of Denmark, 2800 Kongens Lyngby, Denmark

Author contributions: KVC and FGØ conceived and designed the experiments, FGØ, CS and TD performed the experiments, FGØ analysed the data, all authors wrote the manuscript.

Corresponding Author: Freja Gam Østergaard, f.g.ostergaard@rug.nl

Figures: 5 figures and 1 table in main article, no extended data

Number of Words in text: abstract 246 words, introduction 730 words, discussion 1097 words

Funding Sources: This project has received funding from the European Union's Horizon 2020 research and innovation programme under the Marie Sklodowska-Curie grant agreement No 641805. HRS holds a 5-year professorship in precision medicine at the Faculty of Health Sciences and Medicine, University of Copenhagen which is sponsored by the Lundbeck Foundation (Grant Nr. R186-2015-2138).

Conflicts of Interest: Hartwig R. Siebner has received honoraria as speaker from Sanofi Genzyme, Denmark and Novartis, Denmark, as consultant from Lundbeck AS, Denmark and Sanofi Genzyme, Denmark, and as senior editor (NeuroImage) and Editor-in-Chief (Neurimage-Clinical) from Elsevier Publishers, Amsterdam, The Netherlands. He has received royalties as book editor from Springer Publishers, Stuttgart, Germany, and Gyldendal, Copenhagen, Denmark.

Acknowledgements: The authors would like to thank Sascha Gude, Yi He and Milena Kaestner for their technical assistance.

Abstract

Parkinson's disease (PD) is a progressive neurodegenerative disease that is typically diagnosed late in its progression. There is a need for biomarkers suitable for monitoring the disease progression at earlier stages to guide the development of novel neuroprotective therapies. One potential biomarker, α-synuclein, has been found in both the familial cases of PD, as well as the sporadic cases and is considered a key feature of PD. α-synuclein is naturally present in the retina, and it has been suggested that early symptoms of the visual system may be used as a biomarker for PD.

Here, we use a viral vector to induce a unilateral expression of human wildtype α-synuclein in rats as a mechanistic model of protein aggregation in PD. We employed functional magnetic resonance imaging (fMRI) to investigate whether adeno-associated virus (AAV) mediated expression of human wildtype α-synuclein alter functional activity in the visual system. 16 rats were injected with either AAV-α-synuclein (n=7) or AAV-null (n=9) in the *substantia nigra pars compacta* of the left hemisphere. The expression of α-synuclein was validated by a motor assay and post-mortem immunohistochemistry. Five months after the introduction of the AAV-vector, fMRI showed robust blood oxygen level dependent (BOLD) responses to light stimulation in the visual systems of both control and AAV-α-synuclein animals. However, our results demonstrate that the expression of AAV-α-synuclein does not affect functional activation of the visual system. This negative finding suggests that fMRI-based read-outs of visual responses may not be a sensitive biomarker for PD.

Significance statement

We injected an adeno-associated virus (AAV) vector in rats to induce unilateral expression of human wildtype α-synuclein in the substantia nigra, and in the ipsilateral striatum and superior colliculus (SC). This did not affect functional activation of SC as probed with functional MRI. This negative finding

54 discourages the use of functional brain mapping of visually evoked activity as an indicator of regional
55 expression of human α-synuclein.

Introduction

Parkinson's disease (PD) is the second most common neurodegenerative disorder (Wirdefeldt et al., 2011) affecting millions of people worldwide (Thomas and Beal, 2007). Though the disease is primarily considered to be sporadic, there are familial versions caused by a mutation in a single gene (Klein and Westenberger, 2012). These hereditable forms of PD have led to the discovery of several susceptibility genes, such as the *SNCA* gene (park1/4) coding for α-synuclein. Aggregation of α-synuclein into fibrils and Lewy bodies is hypothesized to develop long before the diagnostic symptoms of tremor and postural instability (Noyce et al., 2016). These aggregates have been proposed to give rise to symptoms early in the course of the disease, consequently, they may potentially serve as biomarkers for the progression.

This study focuses on the visual system as several studies have shown that the visual system is affected in PD patients (Davidsdottir et al., 2005; Ekker et al., 2017; Satue et al., 2017). Moreover, these changes have so far failed to provide an unambiguous estimate of disease severity (Ridder et al., 2017). This is likely due to PD being diagnosed at a very late stage of disease progression, where patients are prone to suffer from a wide range of visual changes related to normal aging (Ekker et al., 2017). However, evidence of PD-related changes in vision was provided by *post mortem* studies showing α-synuclein aggregation in the retinae of PD patients (Bodis-Wollner et al., 2014). This finding lead to the hypothesis that α-synuclein aggregation may cause changes in visual responses measured in patients with PD.

A rodent model of α-synuclein expression in the *substantia nigra pars compacta* (SNc), mediated by the adeno-associated virus (AAV) has shown to decrease the number of spines of the dopaminergic cells, which in turn have shown to influence the neuronal firing pattern in the *striatum* (Andersen et al., 2018). In addition to the striatum, the SNc also projects to the *superior colliculus* (SC) which is the primary region for visual processing in rats (Sefton et al., 2014). Further it was shown by Østergaard and colleagues that this model also exhibits changes in the latency of the visual evoked potential (VEP)

measured in the SC (Østergaard et al., 2020). The neuronal firing pattern was measured invasively using electrophysiology making it infeasible to apply in humans. Hence, a non-invasive technique is desirable. Magnetic resonance imaging (MRI) is a non-invasive bioimaging modality, which have been used to investigate regional changes in brain structure of PD patients (Lehéricy et al., 2014). Most MRI-based studies of PD patients have focused on changes in brain structure (Niethammer et al., 2012; Weil et al., 2016). Functional MRI (fMRI) measures the local changes in blood oxygenation related to neuronal activity and has been applied in PD patients to study changes in neuronal function. One of these studies have shown changes in the iron load of cortex and SNc in PD patients (Pyatigorskaya et al., 2014). fMRI may also detect neuronal changes in the dopamine release after a pharmacological challenge in the rodent PD model (Kuebler et al., 2017) also used by Andersen and colleagues (Andersen et al., 2018). This model mimics the mechanistic changes of expressing human wildtype α-synuclein in neurons of the *substantia nigra* (Decressac et al., 2012).

The aim of this study was to use blood-oxygenation level dependent (BOLD) fMRI with a visual flickering full-field illumination stimulation to examine potential functional consequences of expressing human wildtype α-synuclein in the rodent. Adeno-associated virus (AAV) carrying DNA encoding human wildtype α-synuclein (*hSNCA*) was unilaterally injected in SNc in rats with the aim of exogenously expressing the human α-synuclein protein and was thereby expected to cause an asymmetry of the BOLD response. In 2013, Bailey et al. described how the cortex responds differently to frequencies above and below a presentation rate of 10 Hz, therefore we have chosen to use presentation rates of 1Hz and 14 Hz. The response to one frequency could be more sensitive to changes introduced by expressing human α-synuclein compared to the response to the other frequency, as responses to these two frequencies may be governed by different mechanisms (Bailey et al., 2013). We use the regions of interest (ROIs) of the rodent visual system and then compared them to the olfactory bulb (OB). The OB is used as a control region, as this region is easy to define and neutral with regards to visual stimuli.

Methods

Subjects

All animal experiments were carried out in accordance with the European Communities Council Directive (86/609/EEC), and in accordance with Danish law on care of laboratory animals. The protocols were approved by the Danish Animal Experiments Inspectorate (Forsøgsdyrstilsynet) prior to the initiation of the study.

20 female Sprague-Dawley™ (SD) rats (Taconic, Denmark) weighing ~225g (corresponding to ten weeks of age) upon arrival were included in the study. The rats underwent surgery and cylinder test at one test site and were transported to another for MRI scanning. The animals acclimatized to the new housing facility for at least two weeks before imaging. The home cage environment including light cycle, cages and enrichment was similar at the two housing facilities. Both had a 12h:12h light:dark cycle (lights on at 06:00hrs). The cages were enriched with nesting material and a red plastic shelter. Access to food (chow) and water was *ad libitum.*

Surgery

Prior to surgery, each rat was anesthetized using subcutaneous (SC) injections of Hypnorm® (Lundbeck, Valby, Denmark), midazolam 5 mg/ml (B. Braun, Germany), and saline in a 2:1:1 ratio yielding an injection volume of 1.7 ml/kg. The rat was placed in a stereotaxic frame and 0.1 ml Marcain (2.5mg/ml bupivacaine, AstraZeneca, Denmark) was administered locally and subcutaneously (SC) prior to incision. A small craniotomy (Ø=1mm) was made over the *substantia nigra pars compacta* (SNc) of the left hemisphere (AP: -5.5mm; ML: +2.0mm; DV: -7.2mm relative to Bregma (Paxinos and Watson, 1998) to allow for injection of 3 µl adeno-associated virus (AAV) 2/5 ($3x10^{10}$ GC/ml) (Vector biolabs, US), carrying human wildtype α-synuclein (*hSNCA*) using methodology as described by Andersen (Andersen et al.,

2018). Half of the animals acted as controls by having the empty viral vector injected. The animals were post-operatively treated with buprenorphine 0.05 mg/kg every 8th hour for four days. The rats were single-housed after the surgery.

Cylinder test

To validate the expression of human wildtype α-synuclein in the basal ganglia, the rats were tested for motor asymmetry ten weeks after surgery. The animals were recorded with a video camera for five minutes, while they were freely moving in a Plexiglass cylinder. Paw touches on the side of the cylinder were counted offline and blinded to the group. The ratio of touches of contralateral paw to total touches was computed. Animals with an expression of human α-synuclein were hypothesized to use the contralateral paw less than the control animals.

Magnetic Resonance Imaging

Preparation for functional MRI

Five months after the viral injection, the rats were anesthetized and scanned in a 7T Bruker Biospec (Bruker BioSpec 70/20 USR) MRI scanner with an 80 mm radio frequency (RF) transmit quadrature coil and a 20 mm surface receive coil. The surface receive coil was fixed on top of the head using masking tape. The position of the surface ensured good signal coverage of the whole brain having the largest signal sensitivity in the regions of interest: the superior colliculus and visual cortex. Sticky tack (Bantex, South Africa) was placed in the ears of the rats to reduce harmful effects of MR scanner noise during scanning. The animals were scanned at the same time of day, on separate days, to minimize variation caused by the circadian rhythm.

Anaesthesia during scan session

To reduce the unwanted effect of isoflurane on the BOLD signal, we used a combination of low dose isoflurane and dexmedetomidine (Dexdormitor®, Orion Pharma, Finland). Anaesthesia was induced with

isoflurane at 5 % and adjusted to 2.5 % while placing a tail-vein catheter. Subsequently, dexmedetomidine was infused at 0.05 mg/kg/hr (Pawela et al., 2009). When the heart rate decreased to about 200 bpm, isoflurane was adjusted to 0.5 % (in 1 L of oxygen:medical air, 8:2). The animals breathed spontaneously, and the respiration rate of the animals was continuously monitored by a respiration sensor pad (SA Instruments; NY, USA). Blood oxygen saturation and heart rate was monitored transcutaneously using pulse oximetry (Nonin, MN, USA). The core temperature of the animals was monitored with a rectal probe and used as feedback to maintain a constant temperature of 37 °C using heated air (SA Instruments; NY, USA). After one hour of infusion, the infusion rate of dexmedetomidine was increased to 0.1 mg/kg/hr. This concentration is lower than what most literature recommend (Pawela et al., 2009) because the vasoconstrictive effects of dexmedetomidine made measuring SpO2 challenging, and this lower concentration turned out to be sufficient.

MRI protocols

Since the structural T1 weighted is not affected by anaesthesia it was acquired before the fMRI. Before acquiring the actual fMRI, online fMRI correlation analysis was applied at regular time intervals using a visual stimulus paradigm. Online fMRI correlation analysis used the Analysis of Functional NeuroImages (AFNI) software integrated with the fMRI sequence (Cox, 1996). The online fMRI analysis was used to determine when the impact of isoflurane on the neuronal response and BOLD signal was diminished, i.e., washed out. Typically, robust regional BOLD responses were obtained after 180 min.

Structural MRI to be aligned with fMRI included a whole brain 3D T1-weighted fast low angle shot (FLASH) MRI (Repetition time (TR)=1500 ms, Echo time (TE)=8 ms, Inversion time (IR)=103338.0 ms, isotropic 0.2 mm^3 voxels field of view of 175x80x175 mm^3, matrix size=35x16x35).

The echo-planar image (EPI) MRI had an in-plane voxel size of 0.313 x 0.313 mm with slice thickness of 0.500 mm, TR=1500 ms, and TE=8.35 ms, slice gap=0. The Ernst flip angle was determined to 64°, based

on T1 relaxation measurement of cortical grey matter obtained from a separate session (data not shown). 42 coronal slices covered the range from the caudal part of the olfactory bulb to the caudal part of the cerebellum.

Visual stimulation paradigm for fMRI

Visual stimulation was provided by five optical fibres (diameter of 1.5 mm) of "warm white" light provided by a light emitting diode (LED) source placed outside the scanner. The optical fibres were placed in front of the animal head as an array. The light intensity during the stimulation was kept at 20 lx, measured at the level of the eyes using a LED luxmeter (Extech, MA, US).

The stimulation paradigm used a block design that was generated by a micro1401 data acquisition unit (Cambridge Electronic Design Ltd., UK) controlled from Spike2 ver. 7.20 synchronized to TTL triggers from the scanner. The block design included six task blocks per trial repeated five times, where each task block lasted for 21 s, equivalent to 14 TRs. Each task block consisted of either 1 Hz or 14 Hz light flicker. These two frequencies were chosen as one should be just above 10 Hz while the other should be well below, as 10 Hz is considered to be the threshold for saturation of the visual cortex (Van Camp et al., 2006). Between task blocks there were a pause of 14 TRs (21s). The visual stimulation paradigm was repeated five times at each stimulation frequency yielding a total scan time of approximately four hours.

fMRI pre-processing

MRI data were analysed using the FMRIB software library (FSL) (Woolrich et al., 2009). To make a standard brain template, the EPIs were aligned within subject using FMRIB's linear image registration tool (FLIRT) and then averaged across animals to construct a standard brain template. This template was used for registration of the data for later analysis.

Visual inspection caused exclusion of four rats, as these could not be aligned to the standard template leaving 16 to be analysed; nine controls and seven AAV-α-synuclein animals.

Statistical analysis

Functional MRI data were analysed using a three-level statistical analysis pipeline implemented in the FSL expert analysis tool (FEAT). In the first level, the time course of each voxel was fitted with a general linear model (GLM) to produce a statistical map of the z-scores of the correlation for each voxel within each of the scans. Each voxel was corrected for family-wise error with a p-threshold of $p<0.05$. Spatial smoothing was then applied using a Gaussian kernel with full width half maximum of 0.5 mm. In the second level, the z-statistical maps were averaged for each stimulation frequency within each subject yielding two averaged z-statistical maps per animal. Each voxel within the averaged statistical map was corrected for family-wise error with a p-threshold of $p=0.05$. At the third and final level, the averaged statistical maps were averaged within the two groups for each of the two stimulation frequencies. The group statistical maps were compared using an unpaired comparison of the z-statistical maps between the two groups within each frequency paradigm. For visualization, the statistical maps were aligned to the standard brain template (described above) and then superimposed on the high-resolution structural MRI scan.

Structural regions of interest (ROIs) of the superior colliculus and visual cortex were defined manually based on rat brain atlases (Kjonigsen et al., 2015; Papp et al., 2014; Sergejevaa et al., 2015). The olfactory bulb (OB) was used as a control ROI. For each group there were ROIs for OB, right SC, left SC, right VC and left VC. The percent change of the BOLD within the ROIs were extracted from the z-statistical map of each rat using FEAT query. Further, estimation statistics were carried out using the website https://www.estimationstats.com/#/ which is based on the methods described in (Ho et al., 2019). Here the data were compared with the common control method within each stimulus paradigm, tested using a two-sided permutation t-test and corrected for multiple comparisons. The resulting effect sizes and confidence intervals (CI) are listed in table 1.

Immunohistochemistry

At the end of the scan session, the animal was given a bolus 3 ml/kg of Hypnorm® and midazolam was administered SC. The animals were perfusion fixated with intracardial potassium phosphate-buffered saline (KPBS) for three minutes, followed by 4% paraformaldehyde (PFA) premade with methanol. After 10-15 minutes, the rat was decapitated, and the brain extracted. The brain was immersed in 4% PFA for 2 hours, then in phosphate buffer (PBS) with <1% PFA for 24 hours, and finally in KPBS.

Brains were fixed in 30% sucrose for 72 hours before slicing. Once fixed, they were dried and frozen with dry ice and placed in a freezing microtome (Leica CM3050S) for 30 min. 40 µm thick coronal slices were cut and stored in KPBS. All slices were stained within five days.

Brain sections were stained to validate the expression pattern of the human wild type SNCA protein. Before staining, the tissue was quenched with hydrogen peroxide 3 % to remove any traces of blood. The slices were washed and incubated overnight with 4B12 (Thermo Scientific, US) for human α-synuclein as the primary antibody (concentration 1:1000). Subsequently, the slices were washed and incubated with biotin conjugated anti-mouse secondary antibody (Jackson Immunoresearch Laboratories, MA, US) and exposed using a 3,3´-diaminobenzidine (DAB) reaction for approx. 20 minutes. The stained slices were placed on gelatine covered glass slides, and visually examined using a light microscope (Axio scope.A1, Carl Zeiss Microimaging, Germany).

Results

Motor assessment of α-synuclein expression

To validate the expression and impact of human α-synuclein in the rat basal ganglia, α-synuclein and control animals were tested for motor asymmetry in the cylinder test (Andersen et al., 2018). Figure 1A shows the change in the use of the forepaw contralateral to the injection site. Control animals used both paws equally (ratio of 0.5) while α-synuclein animals had a significantly different mean ratio of affected/total touches ratio of 0.35 ($t(14)=2.8$, $p=0.01$). The cylinder test confirmed that the function of the striatum was unilaterally affected in the animals that received the AAV-*hSNCA*-injection, as expected with successful injection of viral particles carrying the *hSNCA*-expressing vector.

Validation of expression of human α-synuclein

Immunohistochemical evaluation carried out after fMRI, showed immunoreactivity towards human α-synuclein in the SNc (Figure 1 E-F), in areas surrounding the SNc, and in the striatum ipsilateral (Figure B-C) to the injection site. Interestingly, small inclusions of immunoreactivity were observed in the optic layer of the ipsilateral superior colliculus (Figure 1G). Minor immunoreactivity was observed along the edges of the tissue (Figure 1 C-D) which were not specific to the injected hemisphere thus considered as unspecific immunoreactivity. Confirmation of α-synuclein in areas ipsilateral to the injected hemisphere supports the observations from the cylinder test.

fMRI of the visual system

The z-statistical maps of the two groups are shown in Figure 2 registered to a high-resolution anatomical scan. Overall, there were detectable responses in both the SC and the VC during light stimulation in both

groups of rats. A modest activation of cerebellar flocculus complex was also observed. This is in line with previous studies where visual stimulation has been applied (Van Camp et al., 2006). Additionally, there was a response in the lateral geniculate nucleus (LGN), as expected (Bailey et al., 2013).

The BOLD changes from each of the ROIs are visualized as points in the top panels of Figure 3 and 4. Figure 3 shows the responses to light flashing at 1 Hz. Estimation statistics comparing each ROI to the OB revealed a significant response in both the VC and SC to the light flashing at 1 Hz (Figure 3). Table 1 lists the full results with effects sizes and confidence intervals (CI). Figure 4 shows the responses to 14 Hz flashing light. There was a statistically significant response to the light stimulation in the SC. Furthermore, a significant difference was shown for VC ipsilateral to the injection of α-synuclein in the 14 Hz condition, with a magnitude of -0.414 (CI[-0.714,-0.182], p=0.0012). However, there was also a difference in the control with an effect size of -0.424 (CI[-0.785,-0.0208],p=0.0496) (Figure 4). Taken together this suggests that the effect was not induced by the expression of α-synuclein. Regardless, this potential asymmetry was explored by comparing the VC within animals with a paired, permutation t-test (Figure 5). The control group showed an insignificant difference between hemispheres measured in the VC effect size of 0.167 (CI[0.0163,0.324], p=0.0932). Similarly, there was no detectable difference between hemispheres in the α-synuclein group effect size -0.156 (CI[-0.268,-0.0296],p=0.064). In conclusion, the expression of the α-synuclein did not induce detectable changes in the BOLD response within animals.

Discussion

This study examined whether expression of α-synuclein in the SNc is associated with abnormal visually evoked brain activation. Using estimation statistics, we found robust BOLD fMRI responses to the visual stimulus in the SC in both control rats and α-synuclein rats. The BOLD response in the VC turned out to be dependent on the presentation rate of the stimulus. A fully developed expression of α-synuclein in the SNc, in the optic layer of SC, and in the striatum did not induce any detectable changes in BOLD fMRI during visual stimulation. This indicates that the level of neuronal activity measured during visual stimulation was not altered by expression of α-synuclein. Alternatively, the scan protocol used for BOLD-fMRI at 7T was not sensitive enough to detect any subtle differences between groups. However, the BOLD responses in rat visual system reproduced the frequency-dependence of the rodent visual cortex that was previously reported (Van Camp et al., 2006). For VC, the visually evoked BOLD responses tended to decrease at stimulation frequencies above 10Hz, similar to the data shown in another study (Bailey et al., 2013). The BOLD signal in the SC did not show this frequency-response behaviour.

The AAV-model was validated both behaviourally and with immunohistochemistry. Previously, asymmetry in the cylinder test have been shown to be specific to α-synuclein expression and is not an effect of induced protein expression with e.g., green fluorescent protein (Andersen et al., 2018). In the present study it is shown that there is indeed asymmetry in the use of forepaws as measured in the cylinder test.

After the scan sessions the brains of each of the animals were stained for human wild type α-synuclein to validate that the model was developed. Both the cylinder test and the immunohistochemistry confirmed a successful development of human α-synuclein expression in the SNc and connected areas such as the striatum and the SC of the α-synuclein animals. Furthermore, it showed that human α-synuclein was present in the SC ipsilateral to the injection, however, this did not cause a detectable

asymmetry in the BOLD-response of the SC upon visual stimulation. Previously, the effect of human α-synuclein expression in rats was measured using *in vivo* electrophysiology. Here, subtle changes in the latency of visual evoked potentials in the SC were shown (Østergaard et al., 2020). The temporal resolution of fMRI might not be suitable to detect subtle increases in latency. This may explain the lack of difference between the responses in the two hemispheres in the α-synuclein animals. There is no direct correlation between event-related potentials and BOLD-fMRI but the γ-band power (Huettel et al., 2004) and event-related spectral perturbations (Engell et al., 2012) have been shown to correlate with the BOLD response. The results in this study supports this discrepancy between the techniques.

Interestingly, there was a significant difference in the VC compared to the OB in the 14 Hz stimulation. A decreased BOLD response was observed in the VC ipsilateral to the injection in the α-synuclein group and in the VC contralateral to the injection in the control group compared to the OB. However, this was not due to asymmetry between the hemispheres in any of the groups, suggesting that the observed effect was not caused by the expression of α-synuclein.

In this study, the rodent eye is not considered to be implicated. Also, the study by Østergaard et al. (Østergaard et al., 2020) did not show any statistically significant changes in the visual cortex after injection of AAV carrying human α-synuclein. If the rodent eye was functionally impacted, then both the SC and the VC would also have been affected. The AAV virus was injected in the SNc and the virus particles tend to spread in the area proximal to the injection site and via direct neuronal projections (Albert et al., 2019). Furthermore, the SNc is not a retinorecipient region of the rat visual system (Sefton et al., 2014).

The AAV α-synuclein rat model of PD is not known to cause large anatomical changes in the brain, however, it does show a loss of dopaminergic cells (Decressac et al., 2012). A study by Kuebler and colleagues suggests that the change in dopamine can be measured by fMRI/PET using an amphetamine

challenge (Kuebler et al., 2017). Generally, the functional consequences of expressing human α-synuclein *in vivo* have been shown with other MR-based methods than BOLD-fMRI. A study using diffusion kurtosis imaging imaged α-synuclein in transgenic mice (Khairnar et al., 2017). This technique evaluates structural changes instead of the changes in oxygen metabolism. Another study used MR-spectroscopy to show that bilaterally overexpressing α-synuclein in the striatum caused changes in energy metabolism in rats (Cuellar-Baena et al., 2016). This technique is sensitive to changes in amounts of metabolites where BOLD detects changes in the oxygen metabolism of larger populations of neurons.

In rodent models of Alzheimer's disease, changes have been reported in functional connectivity patterns at early stages of protein aggregation. This has been observed using resting state fMRI (Grandjean et al., 2014). It can be speculated that this could be caused by protein aggregation and that the specific composition of proteins may be less important. Thus, evaluation of the AAV-model using functional connectivity should be investigated further.

In human patients, Zhao et al. have described changes in the BOLD signal of visual areas concerned with the perception of movement (Zhao et al., 2014). Further studies would be needed to study if motion perception is also affected in the AAV-model. Here, we studied low-level visual processing but higher order functions such as motion perception may be more sensitive to the presence of α-synuclein. Generally, task-related BOLD fMRI is rarely used to study PD in animals and humans. Often resting state fMRI and diffusion MRI are applied (Lehericy et al., 2017; Tessitore et al., 2019).

The necessity of anaesthesia is a major challenge for fMRI studies in rodents. Anaesthesia generally works by altering the neuronal activity (Masamoto and Kanno, 2012). Consequently, it will also affect the BOLD response. Unlike urethane and alpha-chloralose, a mix of isoflurane and dexmedetomidine may be used in longitudinal studies. The anaesthesia paradigm used in the present study showed detectable and robust activation of the SC three hours after the induction of anaesthesia. As the

functional changes in the SC are believed to be subtle, it cannot be ruled out that the effect of the anaesthesia may mask potential functional differences.

In summary, this study shows that the fully developed expression of α-synuclein in the SNc along with the optic layer of SC and the striatum, did not induce any asymmetry detectable using BOLD fMRI during visual stimulation.

References

Albert, K., Voutilainen, M.H., Domanskyi, A., Piepponen, T.P., Ahola, S., Tuominen, R.K., Richie, C., Harvey, B.K., Airavaara, M., 2019. Downregulation of tyrosine hydroxylase phenotype after AAV injection above substantia nigra: Caution in experimental models of Parkinson's disease. J. Neurosci. Res. 97, 346–361. https://doi.org/10.1002/jnr.24363

Andersen, M.A., Christensen, K.V., Badolo, L., Smith, G.P., Jeggo, R., Jensen, P.H., Andersen, K.J., Sotty, F., 2018. Parkinson's disease-like burst firing activity in subthalamic nucleus induced by AAV-α-synuclein is normalized by LRRK2 modulation. Neurobiol. Dis. 116, 13–27. https://doi.org/10.1016/j.nbd.2018.04.011

Bailey, C.J., Sanganahalli, B.G., Herman, P., Blumenfeld, H., Gjedde, A., Hyder, F., 2013. Analysis of time and space invariance of BOLD responses in the rat visual system. Cereb. Cortex 23, 210–222. https://doi.org/10.1093/cercor/bhs008

Bodis-Wollner, I., Kozlowski, P.B., Glazman, S., Miri, S., 2014. a-Synuclein in the Inner Retina in Parkinson Disease. Ann. Neurol. 75, 964–966. https://doi.org/10.1002/ana.24182

Cox, R.W., 1996. AFNI : Software for Analysis and Visualization of Functional Magnetic Resonance Neuroimages. Comput. Biomed. Res. 29, 162–173. https://doi.org/10.1006/cbmr.1996.0014

Cuellar-Baena, S., Landeck, N., Sonnay, S., Buck, K., Mlynarik, V., In 'T Zandt, R., Kirik, D., 2016. Assessment of brain metabolite correlates of adeno-associated virus-mediated over-expression of human alpha-synuclein in cortical neurons by in vivo 1H-MR spectroscopy at 9.4 T. J. Neurochem. 137, 806–819. https://doi.org/10.1111/jnc.13547

Davidsdottir, S., Cronin-Golomb, A., Lee, A., 2005. Visual and spatial symptoms in Parkinson's disease. Vision Res. 45, 1285–1296. https://doi.org/10.1016/j.visres.2004.11.006

Decressac, M., Mattsson, B., Lundblad, M., Weikop, P., Björklund, A., 2012. Progressive neurodegenerative and behavioural changes induced by AAV-mediated overexpression of α-synuclein in midbrain dopamine neurons. Neurobiol. Dis. 45, 939–953. https://doi.org/10.1016/j.nbd.2011.12.013

Ekker, M.S., Janssen, S., Seppi, K., Poewe, W., de Vries, N.M., Theelen, T., Nonnekes, J., Bloem, B.R., 2017. Ocular and visual disorders in Parkinson's disease: Common but frequently overlooked. Park. Relat. Disord. 40, 1–10. https://doi.org/10.1016/j.parkreldis.2017.02.014

Engell, A.D., Huettel, S., McCarthy, G., 2012. The fMRI BOLD signal tracks electrophysiological spectral perturbations, not event-related potentials. Neuroimage 59, 2600–2606. https://doi.org/10.1016/j.neuroimage.2011.08.079

Grandjean, J., Schroeter, A., He, P., Tanadini, M., Krstic, D., Keist, R., Konietzko, U., Klohs, J., Nitsch, R.M., Rudin, M., 2014. Early Alterations in Functional Connectivity and White Matter Structure in a Transgenic Mouse Model of Cerebral Amyloidosis. J. Neurosci. 34, 13780–13789. https://doi.org/10.1523/jneurosci.4762-13.2014

Ho, J., Tumkaya, T., Aryal, S., Choi, H., Claridge-Chang, A., 2019. Moving beyond P values: data analysis with estimation graphics. Nat. Methods 16, 565–566. https://doi.org/10.1038/s41592-019-0470-3

394 Huettel, S.A., McKeown, M.J., Song, A.W., Hart, S., Spencer, D.D., Allison, T., McCarthy, G., 2004. Linking
395 Hemodynamic and Electrophysiological Measures of Brain Activity: Evidence from Functional MRI
396 and Intracranial Field Potentials. Cereb. Cortex 14, 165–173.
397 https://doi.org/10.1093/cercor/bhg115

398 Khairnar, A., Ruda-Kucerova, J., Szabó, N., Drazanova, E., Arab, A., Hutter-Paier, B., Neddens, J., Latta, P.,
399 Starcuk, Z., Rektorova, I., 2017. Early and progressive microstructural brain changes in mice
400 overexpressing human α-Synuclein detected by diffusion kurtosis imaging. Brain. Behav. Immun. 61,
401 197–208. https://doi.org/10.1016/j.bbi.2016.11.027

402 Kjonigsen, L.J., Lillehaug, S., Bjaalie, J.G., Witter, M.P., Leergaard, T.B., 2015. Waxholm Space atlas of the
403 rat brain hippocampal region: Three-dimensional delineations based on magnetic resonance and
404 diffusion tensor imaging. Neuroimage 108, 441–449.
405 https://doi.org/10.1016/j.neuroimage.2014.12.080

406 Klein, C., Westenberger, A., 2012. Genetics of Parkinson's Disease. Cold Spring Habor Perspect. Med. 2,
407 1–15. https://doi.org/10.1016/j.jconrel.2014.05.021

408 Kuebler, L., Herfert, K., Landeck, N., Maurer, A., Amend, M., Thielcke, A., Buss, S., Marciano, S., Stumm,
409 R., Wehrl, H.F., Kirik, D., Pichler, B.J., 2017. Quantification of molecular and functional changes in a
410 rat model of Parkinson's disease using a simultaneaous PET/fMRI protocol.

411 Lehéricy, S., Bardinet, E., Poupon, C., Vidailhet, M., François, C., 2014. 7 tesla magnetic resonance
412 imaging: A closer look at substantia nigra anatomy in Parkinson's disease. Mov. Disord. 29, 1574–
413 1581. https://doi.org/10.1002/mds.26043

414 Lehericy, S., Vaillancourt, D.E., Seppi, K., Monchi, O., Rektorova, I., Antonini, A., McKeown, M.J., Masellis,
415 M., Berg, D., Rowe, J.B., Lewis, S.J.G., Williams-Gray, C.H., Tessitore, A., Siebner, H.R., 2017. The
416 role of high-field magnetic resonance imaging in parkinsonian disorders: Pushing the boundaries
417 forward. Mov. Disord. 32, 510–525. https://doi.org/10.1002/mds.26968

418 Masamoto, K., Kanno, I., 2012. Anesthesia and the quantitative evaluation of neurovascular coupling. J.
419 Cereb. Blood Flow Metab. 32, 1233–1247. https://doi.org/10.1038/jcbfm.2012.50

420 Niethammer, M., Feigin, A., Eidelberg, D., 2012. Functional neuroimaging in Parkinson's disease. Cold
421 Spring Harb. Perspect. Med. 2, 1–21. https://doi.org/10.1101/cshperspect.a009274

422 Noyce, A.J., Lees, A.J., Schrag, A.-E., 2016. The prediagnostic phase of Parkinson's disease. J. Neurol.
423 Neurosurg. Psychiatry 87, 871–878. https://doi.org/10.1136/jnnp-2015-311890

424 Østergaard, F.G., Himmelberg, M.M., Laursen, B., Siebner, H.R., Wade, A.R., Christensen, K.V., 2020.
425 Classification of α-synuclein-induced changes in the AAV α-synuclein rat model of Parkinson's
426 disease using electrophysiological measurements of visual processing. Sci. Rep. 10, 1–14.
427 https://doi.org/10.1038/s41598-020-68808-3

428 Papp, E.A., Leergaard, T.B., Calabrese, E., Johnson, G.A., Bjaalie, J.G., 2014. Waxholm Space atlas of the
429 Sprague Dawley rat brain. Neuroimage 97, 374–386.
430 https://doi.org/10.1016/j.neuroimage.2014.04.001

431 Pawela, C.P., Biswal, B.B., Hudetz, A.G., Schulte, M.L., Li, R., Jones, S.R., Cho, Y.R., Matloub, H.S., Hyde,
432 J.S., 2009. A protocol for use of medetomidine anesthesia in rats for extended studies using task-

induced BOLD contrast and resting- state functional connectivity. Neuroimage 46, 1137–1147. https://doi.org/10.1016/j.neuroimage.2009.03.004

Paxinos, G., Watson, C., 1998. The Rat Brain: in stereotaxic Coordinates, 4th ed. Academic Press, An imprint of Elsevier, San Diego, London.

Pyatigorskaya, N., Gallea, C., Garcia-Lorenzo, D., Vidailhet, M., Lehericy, S., 2014. A review of the use of magnetic resonance imaging in Parkinson's disease. Ther. Adv. Neurol. Disord. 7, 206–220. https://doi.org/10.1177/1756285613511507

Ridder, A., Müller, M.L.T.M., Kotagal, V., Frey, K.A., Albin, R.L., Bohnen, N.I., 2017. Impaired contrast sensitivity is associated with more severe cognitive impairment in Parkinson disease. Park. Relat. Disord. 34, 15–19. https://doi.org/10.1016/j.parkreldis.2016.10.006

Satue, M., Rodrigo, M.J., Obis, J., Vilades, E., Gracia, H., Otin, S., Fuertes, M.I., Alarcia, R., Crespo, J.A., Polo, V., Larrosa, J.M., Pablo, L.E., Garcia-Martin, E., 2017. Evaluation of progressive visual dysfunction and retinal degeneration in patients with parkinson's disease. Investig. Ophthalmol. Vis. Sci. 58, 1151–1157. https://doi.org/10.1167/iovs.16-20460

Sefton, A.J., Dreher, B., Harvey, A.R., Martin, P.R., 2014. Visual System, The Rat Nervous System: Fourth Edition. https://doi.org/10.1016/B978-0-12-374245-2.00030-9

Sergejevaa, M., Papp, E.A., Bakker, R., Gaudneka, M.A., Okamura-Ohoe, Y., Bolinef, J., Bjaalieb, J.G., Andreas, H., 2015. Anatomical landmarks for registration of experimental image data to volumetric rodent brain atlasing templates. J. Neurosci. Methods 240, 161–169. https://doi.org/10.1016/j.jneumeth.2014.11.005

Tessitore, A., Cirillo, M., De Micco, R., 2019. Functional Connectivity Signatures of Parkinson's Disease. J. Parkinsons. Dis. 9, 637–652. https://doi.org/10.3233/JPD-191592

Thomas, B., Beal, M.F., 2007. Parkinson's disease. Hum. Mol. Genet. 16, R183–R194. https://doi.org/10.1007/978-1-4939-7880-9_5

Van Camp, N., Verhoye, M., De Zeeuw, C.I., Van der Linden, A., 2006. Light Stimulus Frequency Dependence of Activity in the Rat Visual System as Studied With High-Resolution BOLD fMRI. J. Neurophysiol. 95, 3164–3170. https://doi.org/10.1152/jn.00400.2005

Weil, R.S., Schrag, A.E., Warren, J.D., Crutch, S.J., Lees, A.J., Morris, H.R., 2016. Visual dysfunction in Parkinson's disease. Brain 139, 2827–2843. https://doi.org/10.1093/brain/aww175

Wirdefeldt, K., Adami, H., Cole, P., Trichopoulos, D., Mandel, J., 2011. Epidemiology and etiology of Parkinson ' s disease : a review of the evidence. Eur. J. Epidemiol. 26, S1–S58. https://doi.org/10.1007/s10654-011-9581-6

Woolrich, M.W., Jbabdi, S., Patenaude, B., Chappell, M., Makni, S., Behrens, T., Beckmann, C., Jenkinson, M., Smith, S.M., 2009. Bayesian analysis of neuroimaging data in FSL. Neuroimage 45, S173–S186. https://doi.org/10.1016/j.neuroimage.2008.10.055

Zhao, Y., Zheng, X., Wang, Q., Xu, J., Xu, X., Zhang, M., 2014. Altered activation in visual cortex: unusual functional magnetic resonance imaging finding in early Parkinson's disease. J. Int. Med. Res. 42, 503–15. https://doi.org/10.1177/0300060513507647

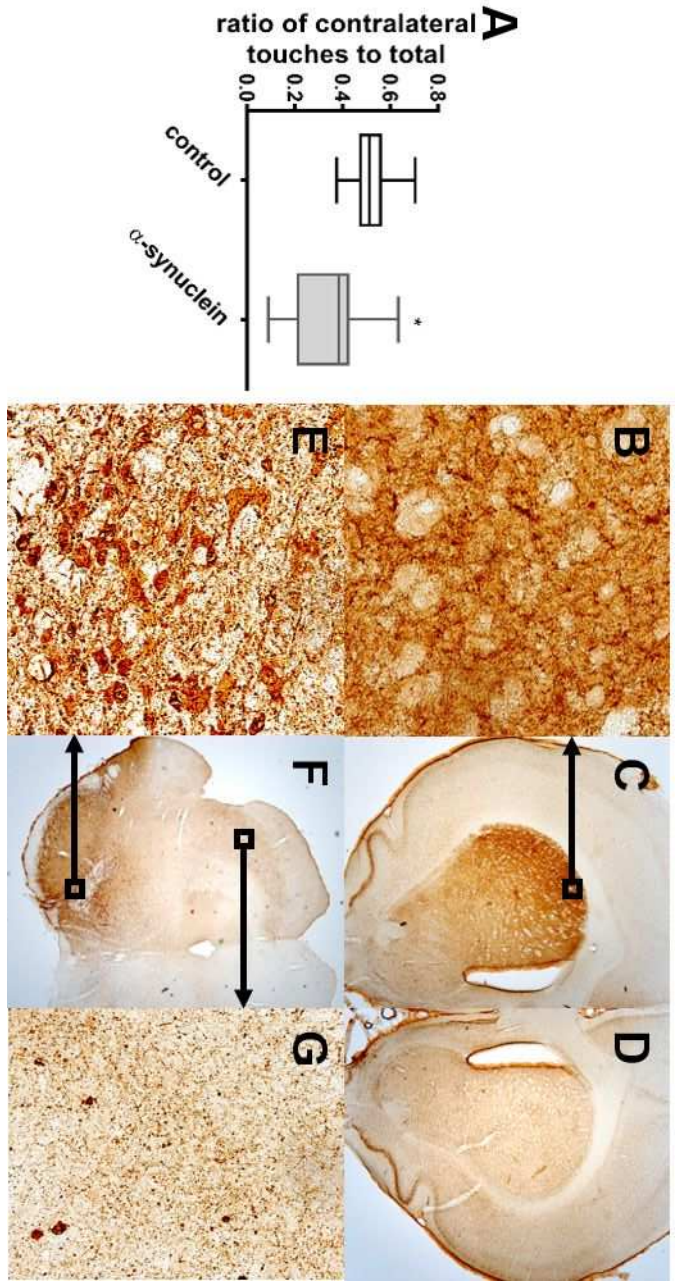

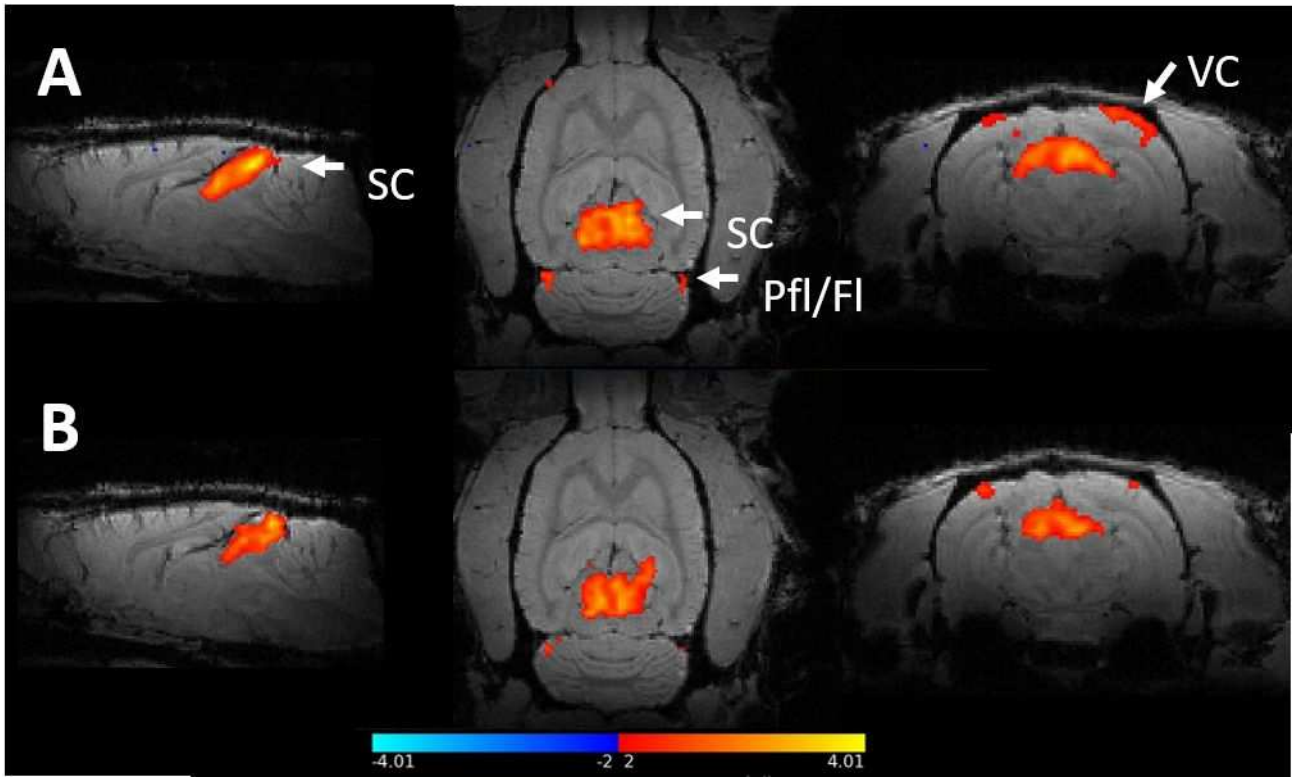

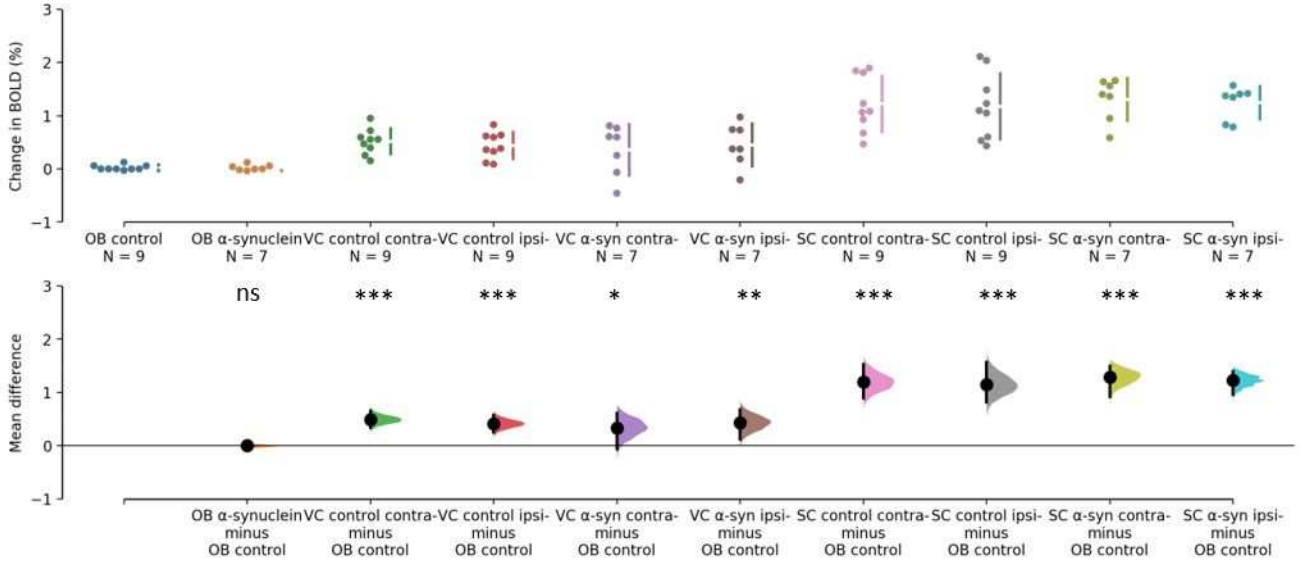

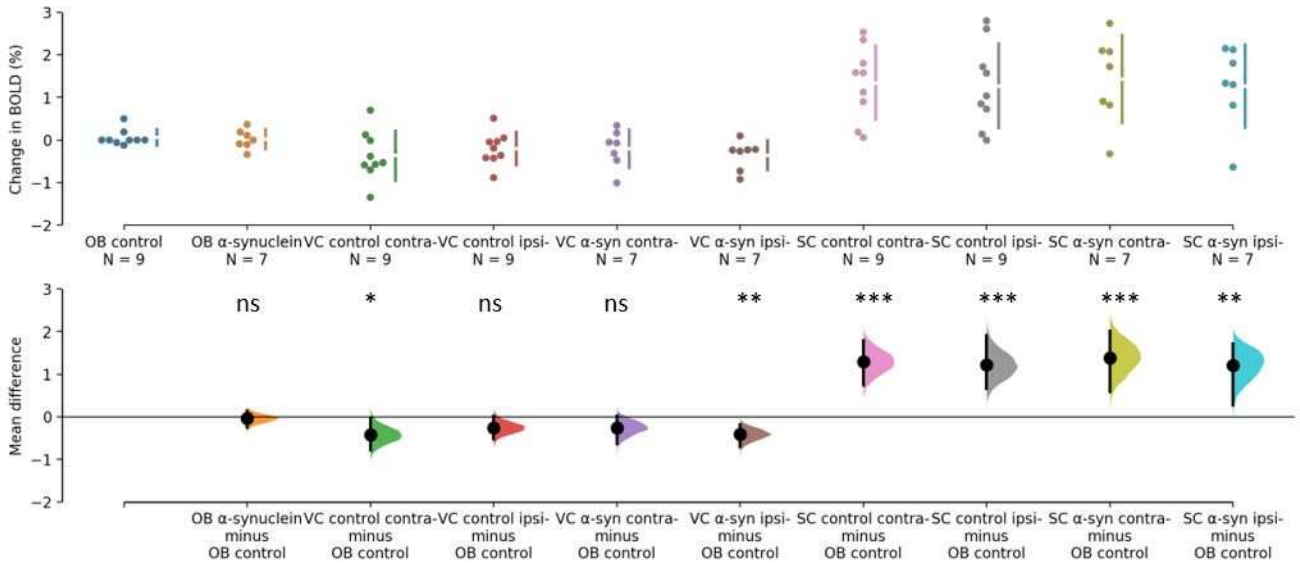

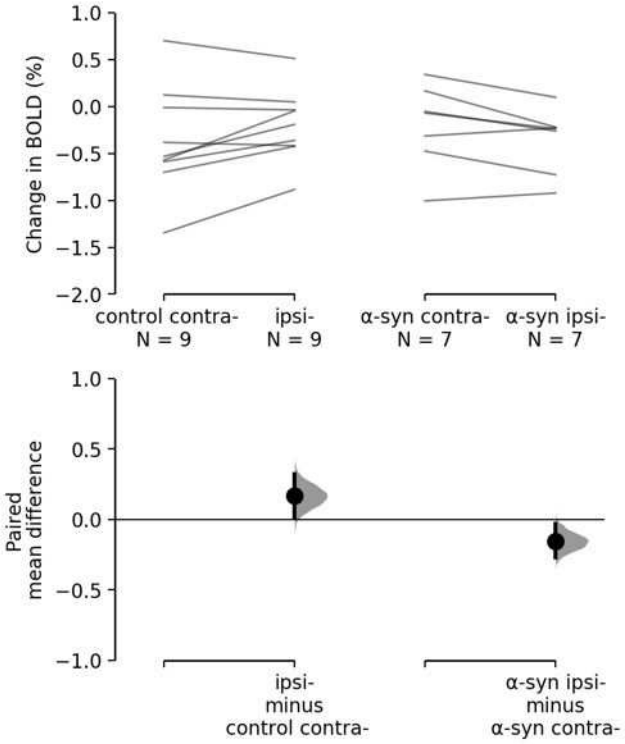

Table 1

Figure	Stimulus	Control ROI	ROI	Effect size	CI (width 95.0 %)		p-value
					Lower bound	Upper bound	
3	1 Hz	OB control	OB α-synuclein	-0.000905	-0.00444	0.0502	0.981
			VC control contra-	0.493	0.344	0.651	0.00022
			VC control ipsi-	0.415	0.255	0.568	0.00099
			VC α-synuclein contra-	0.336	-0.0667	0.609	0.0452
			VC α-synuclein ipsi-	0.429	0.127	0.68	0.0044
			SC control contra-	1.2	0.885	1.52	0.000123
			SC control ipsi-	1.15	0.816	1.57	0.000498
			SC α-synuclein contra-	1.28	0.917	1.5	0.000133
			SC α-synuclein ipsi-	1.22	0.958	1.4	0.000036
4	14 Hz	OB control	OB α-synuclein	-0.038	-0.243	0.14	0.722
			VC control contra-	-0.424	-0.785	-0.0208	0.0496
			VC control ipsi-	-0.257	-0.528	0.0135	0.0926
			VC α-synuclein contra-	-0.258	-0.638	0.0227	0.139
			VC α-synuclein ipsi-	-0.414	-0.714	-0.182	0.0012
			SC control contra-	1.29	0.744	1.8	0.0006
			SC control ipsi-	1.22	0.66	1.9	0.0006
			SC α-synuclein contra-	1.38	0.585	2.01	0.001
			SC α-synuclein ipsi-	1.21	0.273	1.72	0.0026